# Chemistry of ruthenium(II) complexes of N-substituted 1,2-benzoquinone diimines. Synthesis, structure and redox properties ‡

Kedar Nath Mitra,[a] Subrata Choudhury,[a] Alfonso Castiñeiras[b] and Sreebrata Goswami *,†,[a]

[a] *Department of Inorganic Chemistry, Indian Association for the Cultivation of Science, Calcutta 700 032, India*
[b] *Departamento de Quimica Inorganica, Facultad de Farmacia, Universidad de Compostela, 15706-Santiago de Compostela, Spain*

A series of ruthenium complexes of *N*-aryl-1,2-benzoquinone diimine chelates [Ru(acac)₂L] have been isolated *via* ruthenium promoted oxidative dimerization of arylamines. These compounds were obtained from the reaction of [Ru(acac)₃] and arylamines. The crystal structure of one representative case has been determined to authenticate the formation of the compound from a heretofore unknown chemical transformation. The structural data revealed a planar diimine L. The two C–N (imine) and two conjugate C–C double bonds in the quinonoid ring are localized and are indicative of the bivalent state of the metal ion. A plausible reaction pathway is discussed. Extended Hückel calculations on [Ru(acac)₂L] revealed that the metal–ligand overlap is high. The electronic transitions of the complexes are discussed based on the frontier MO diagram. There are multiple transitions in the range 1100 to 250 nm. The highly intense transition at *ca.* 520 nm has been assigned to a transition involving two heavily mixed metal–ligand orbitals. The diimine complexes undergo four successive one electron transfer processes. Two are metal centered, occurring at positive potentials, and two are ligand reductions at negative potentials. The $E°_{298}$ values of all the four redox processes are dependent on the nature of substitution of the quinone diimine ligand. The structure and physicochemical properties of these complexes are compared with those of [Ru(acac)₂(bqdi)] (bqdi = *o*-benzoquinone diimine) obtained from the reaction of [Ru(acac)₃] and *o*-phenylenediamine.

Ruthenium complexes of quinone related *o*-benzoquinone diimine ligands are of interest[1–10] in contemporary research. These ligands are redox active, and can be reduced to semi-quinone diimine and further to diamine forms. Thus, there are different possibilities of charge distributions in the complexes of these ligands with the redox active metal ions due to the high degree of orbital mixing between metal and ligand orbitals. Herein we describe a family of ruthenium complexes of *N*-aryl-1,2-benzoquinone diimines (L). The ligands are formed *in situ* presumably *via* template synthesis on ruthenium [equation (1); R′ = aryl].

$$[Ru(acac)_3] \xrightarrow[\text{heat}]{R'NH_2} [Ru(acac)_2L] \qquad (1)$$
$$\mathbf{1}$$
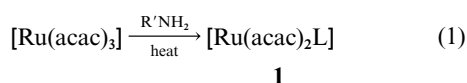
Previous studies on ruthenium quinone diimines have largely been confined to complexes of symmetrical diimines[1,6,8] derived from 1,2-phenylenediamine, and 9,10-phenanthrenequinone diimines. An example of ethylenediimine was reported[11] which formed by the oxidative dehydrogenation of co-ordinated ethylenediamine. It may be noted here that unsymmetrical diimines of the above type are not directly achievable from arylamines and the ruthenium compounds, **1**, involving unsymmetrically N-substituted diimines were not known. The physicochemical properties of the above ruthenium compounds are reported and are compared with those of a related system. The ease with which the reaction occurs and the rich redox behaviour of the resultant complexes are an indication of the potentially novel chemistry that these diimines may engender in the area of tran-
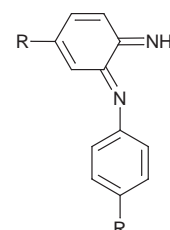
| R | L |
|---|---|
| H | L¹ |
| Me | L² |
| OMe | L³ |
| Cl | L⁴ |

sition metal diimine complexes. A preliminary account on the formation of a member of the [Ru(acac)₂L] series has recently been reported by us.[12]

## Results and discussion

### The reaction

The synthetic reaction (1) involves heating a mixture of [Ru(acac)₃] (0.25 g) and an aromatic amine, R′NH₂ (0.5 g), at 130 °C on an oil-bath for 1.5 h. Chromatographic purification followed by crystallization yielded dark brown needles of [Ru(acac)₂L] in *ca.* 30% yield. The reaction became much faster (30 min) and there was a notable increase of the yield of **1** (*ca.* 70%) on addition of a few drops of NEt₃ at the initial stage. The reaction occurs only neat and in air.

The mechanism of reaction (1) is complex and not yet known. The overall transformation, R′NH₂ to L [equation (2)],

$$2R'NH_2 \longrightarrow L + 4e^- + 4H^+ \qquad (2)$$
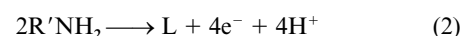
is a combination of two major processes. Oxidative *ortho*

**Table 1** Characterization data

| Compound | IR[a]/cm⁻¹ | | ¹H NMR[b] (δ) | | | |
|---|---|---|---|---|---|---|
| | $\nu$(N–H) | $\nu$(C–N) | Me (acac) | Me (L) | CH (acac) | NH |
| **1a** | 3230 | 1580 | 1.76, 1.83, 2.35 | | 5.10, 5.39 | 10.77 |
| **1b** | 3220 | 1580 | 1.76, 1.83, 1.85, 2.37 | 2.32, 2.44 | 5.13, 5.37 | 10.85 |
| **1c** | 3220 | 1580 | 1.77, 1.82, 1.85, 2.34 | 3.64, 3.86 | 5.16, 5.43 | 10.89 |
| **1d** | 3200 | 1580 | 1.79, 1.86, 1.92, 2.35 | | 5.15, 5.41 | 11.01 |
| **2** | 3280 | 1585 | 1.77, 2.40 | | 5.45 | 10.49 |

[a] As KBr disc. [b] In CDCl₃; SiMe₄ as internal standard; aromatic proton resonances occur in the region δ 6.5–7.4.

dimerization of R′NH₂ and further oxidation of the resultant dimer would form the diimine ligand, L. Anodic oxidations of aromatic amines[13] followed by *para* coupling leading to *p*-benzidine or *p*-semidine (*N*-phenylbenzene-1,4-diamine) are common. There are also examples of oxidation of R′NH₂ to the diazo compound R′N=NR′. The oxidative *ortho* coupling of R′NH₂ leading directly to *o*-semidine, however, was not known. It may be noted here that substitution of one acac⁻ and subsequent *cis* co-ordination of R′NH₂ residues (or their deprotonated form) to two *cis* vacant sites of ruthenium would bring the two interacting R′NH₂ sites in close proximity for *ortho* dimerization. The reaction, under consideration, does not occur in the absence of O₂. Ruthenium promoted oxidation of amines to imines by O₂ is documented.[14] It is, therefore, believed that the oxidation reaction, for the formation of L, presumably occurs *via* aerial oxidation. Furthermore, reaction (2) is associated with the release of four protons and addition of NEt₃, which acts as a proton sink, facilitates this. Interestingly and expectedly, the di-*ortho*-substituted aniline, 2,6-dimethylaniline, does not react under similar conditions. The present example of oxidative dimerization of R′NH₂ in the presence of [Ru(acac)₃] has resulted in a series of unsymmetrical N-substituted diimines, the co-ordination chemistry of which is unprecedented in the literature. Very recently, some osmium complexes, obtained from a similar reaction, have been reported by us.[15]

In order to compare the physicochemical properties of the above ruthenium diimines, one closely related compound, *viz*. [Ru(acac)₂(bqdi)] **2** (bqdi = *o*-benzoquinone diimine) was synthesized in moderate yield (40%) from the reaction of [Ru(acac)₃] and *o*-phenylenediamine in 2-methoxyethanol. The compound was purified by column chromatography and obtained as brown needles.

### Formulation and spectroscopic characterization

Both the compounds **1** and **2** gave satisfactory analyses (Experimental section). They are soluble in common organic solvents and are diamagnetic. Selected spectral data are collected in Table 1. The N–H stretch occurs[16] as a sharp feature of moderate intensity in the range 3340–3370 cm⁻¹. The presence of a strong C=N stretch[17] near 1600 cm⁻¹ characterizes the diimine chromophore in the compound. The ¹H NMR spectral data are of interest. The characteristic proton resonances are: (i) the methyl protons which appear as singlets occur in the range δ 1.75 to 3.90; (ii) resolved aromatic proton resonances between δ 6.5 and 7.4 and (iii) the imine proton appears as a broad singlet[6] (width at half height 0.06 ppm). The shifts of δ which are observed in the proton resonances, within this series of complexes, can be attributed to the nature of the substituents. Thus, the imine resonance was shifted furthest upfield for the electron-donating methoxy substituent and furthest downfield for the electron-withdrawing chloride substituent. The bqdi complex, **2**, is symmetrical ($C_2$) and displayed a much simpler spectrum.

The electronic spectral data are collected in Table 2. The spectrum of a typical [Ru(acac)₂L] **1** complex is displayed in

**Table 2** Electronic spectral data

| Compound | $\lambda_{max}$/nm[a] ($\varepsilon$/M⁻¹ cm⁻¹) | | | |
|---|---|---|---|---|
| **1a** | 275 (24 550) | 320[b] (10 720) | 519 (19 050) | 1025[c] (90) |
| **1b** | 270 (28 180) | 325[b] (11 220) | 522 (17 780) | 1000[c] (123) |
| **1c** | 270 (25 120) | 320[b] (10 960) | 524 (21 880) | 975[c] (135) |
| **1d** | 270 (26 300) | 330[b] (12 300) | 520 (15 490) | 1100[c] (90) |
| **2** | 265 (16 980) | 300[b] (7080) | 500 (6760) | 950[c] (60) |

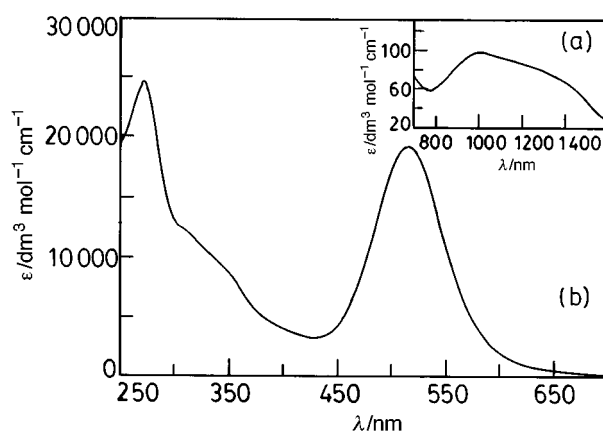[a] Spectra were obtained in acetonitrile. [b] Shoulder. [c] Associated with an ill defined shoulder at lower energy.



**Fig. 1** Electronic spectrum of complex **1a** (L = L¹) in MeCN: (a) 1600–700, (b) 700–250 nm

Fig. 1. The lowest energy transition, associated with an ill defined shoulder, occurring in the near-IR region is weak and very broad. The energy of this transition shifts to the red as the acceptor character of the quinone diimine ligand increases. Notably, the low energy transition in the present complexes occurs at lower energy compared to that in a related 2,2′-bipyridine (bpy) complex. In an attempt to obtain some insight into the nature of the orbitals involved in the electronic transitions an EHMO calculation has been performed on the compound [Ru(acac)₂L¹] **1a** making use of the CACAO program by Mealli and Proserpio.[18] The calculation was performed on the basis of atomic positions obtained from the crystal data analysis of **1a**. The symmetry point group is $C_1$. The partial MO interaction diagram is shown in Fig. 2. Thus the ruthenium t₂g orbitals interact with the orbitals of the diimine ligand to form LUMO, HOMO, HOMO-1 and HOMO-2 molecular orbitals. Interestingly, the two molecular orbitals, *viz*. LUMO and HOMO-2 are heavily mixed orbitals whereas HOMO and HOMO-1 are almost pure metal orbitals. Pictorial representation of these four molecular orbitals are deposited as SUP 57411. Thus, the low energy transition and its associated shoulder may be assigned[1–3,19] to transitions from the nonbonding HOMO and HOMO-1 to the LUMO. The next highly intense band in the spectrum of **1** is assigned[3,20] to a transition between two heavily mixed metal–ligand orbitals, LUMO and HOMO-2. The spectrum of [Ru(acac)₂(bqdi)] **2** is of similar

**Table 3** Selected bond distances (Å) and angles (°) and their estimated standard deviations for complexes **1a**·0.25H$_2$O and **2**

[Ru(acac)$_2$L$^1$]·0.25H$_2$O

| | | | |
|---|---|---|---|
| Ru(1)–N(31) | 1.946(5) | Ru(2)–N(61) | 1.930(5) |
| Ru(1)–N(36) | 1.997(5) | Ru(2)–N(66) | 2.008(5) |
| Ru(1)–O(11) | 2.018(5) | Ru(2)–O(51) | 2.050(4) |
| Ru(1)–O(13) | 2.030(5) | Ru(2)–O(53) | 2.029(5) |
| Ru(1)–O(21) | 2.050(4) | Ru(2)–O(43) | 2.065(5) |
| Ru(1)–O(23) | 2.067(4) | Ru(2)–O(41) | 2.046(5) |
| | | | |
| N(31)–Ru(1)–N(36) | 78.9(2) | N(61)–Ru(2)–N(66) | 79.6(2) |
| O(11)–Ru(1)–N(36) | 91.3(2) | O(51)–Ru(2)–O(53) | 91.6(2) |
| O(23)–Ru(1)–O(21) | 90.7(2) | O(41)–Ru(2)–O(43) | 89.6(2) |

[Ru(acac)$_2$(bqdi)] **2**

| | | | |
|---|---|---|---|
| Ru(1)–N(1) | 1.958(2) | Ru(1)–O(2) | 2.0748(17) |
| Ru(1)–O(1) | 2.0328(16) | | |
| | | | |
| N(1)–Ru(1)–N(1a) | 79.09(13) | O(1)–Ru(1)–O(2) | 89.37(6) |



**Fig. 3** Perspective view of the molecule **A** of compound **1a** showing the atom numbering scheme and the co-ordination geometry about the ruthenium atom. Thermal ellipsoids enclose 50% of the electron density. Hydrogen atoms are drawn with an arbitrary $B_{iso} = 1.5$ Å$^2$ and represented by open circles



**Fig. 2** Partial energy level diagram obtained from an extended Hückel calculation on [Ru(acac)$_2$L$^1$]



**Fig. 4** Perspective view of the molecule **2** showing the atom numbering scheme and the co-ordination geometry about ruthenium. Details as in Fig. 3.

type to that of **1** in respect of the number of bands and shape but differs in transition energies. In general, the energy of the transitions in **2** are higher than the corresponding ones in **1** which may be attributed to the presence of a lower energy acceptor orbital in **1**. The higher π-acceptor ability of L over bqdi has also been reflected in the electrochemical data (see below).

The rest of the transitions in complexes **1** and **2** occurring in the UV region are either intraligand transitions or involve metal and higher energy ligand orbitals and are not considered here.

**Crystal structure**

Compounds **1a** and **2** formed suitable X-ray quality crystals the structures of which were determined. Suitable crystals of **1a** were obtained by slow evaporation of a solution of [Ru(acac)$_2$-L$^1$] in hexane. The molecule contained 0.25 water as solvate which possibly comes from the solvent used for crystallization. The asymmetric unit consists of two crystallographic distinct molecules. The co-ordination sphere involves RuO$_4$N$_2$. The metal is co-ordinated in a distorted octahedral geometry by the four oxygens of two acetylacetonate ligands oriented in a *cis* geometry and by the two nitrogens of a diimine ligand. A
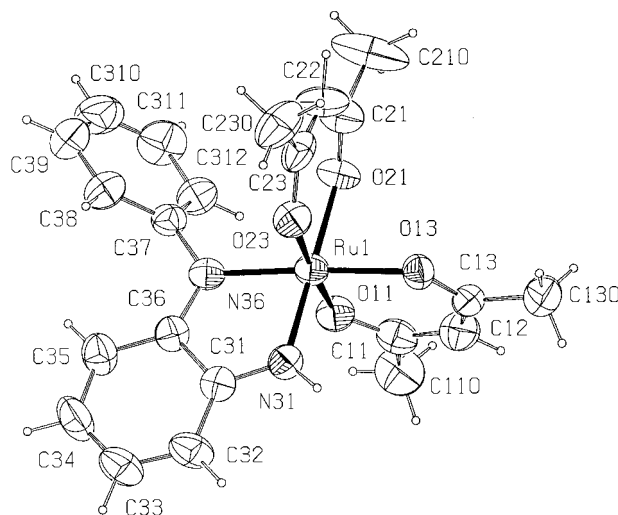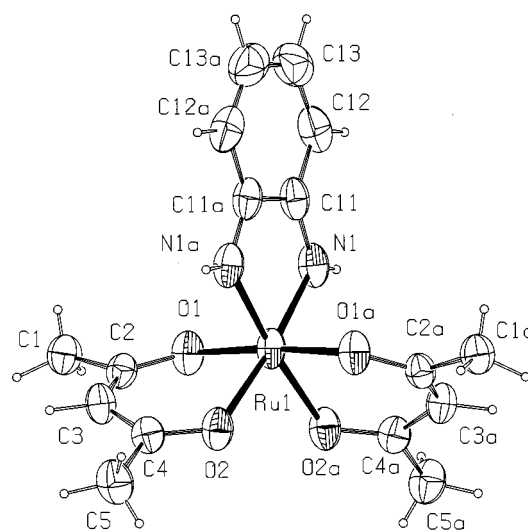
view of one of the two molecules (**A**) is shown in Fig. 3. Selected bond parameters are collected in Table 3. The imine C–N bond lengths, average 1.335(8) Å, are within the range expected[7,9,17,21,22] for a diimine oxidation state of L. These imine bonds are considerably shorter than the C–N single bond, *viz.* C(37)–N(36) (molecule **A**) and C(67)–N(66) (molecule **B**), average 1.433(8) Å. Moreover, the C–C bond lengths [average 1.356(10) Å] at positions that would have localized double bonds for the diimine form, for example C(34)–C(35) and C(32)–C(33) bonds in molecule **A**, are significantly shorter than the other C–C lengths [average 1.422(9) Å] of the same ring. Furthermore, four atoms of the diimine chelate and ruthenium are planar with no atom deviating by more than 0.01 Å from the mean plane.

The crystals of complex **2** for X-ray crystallography were obtained by slow diffusion of hexane into a dichloromethane solution of the compound. A molecular view with the atomic numbering scheme is displayed in Fig. 4. Table 3 contains selected bond distances and angles. The molecule possesses $C_2$ symmetry. The twofold axis of symmetry passes through Ru(1) bisecting the bonds C(11)–C(11a) and C(13)–C(13a). Thus the
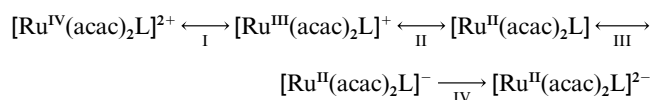
asymmetric unit consists of half the molecule and the other half was generated by the twofold axis. The characteristics of the structure are: (a) short Ru–N distances, (b) long C–N lengths, (c) localized double bond character of C(12)–C(13) and C(12a)–C(13a) bonds in the quinonoid ring and (d) ruthenium and four atoms of the chelate, *viz.* N(1), C(11), C(11a), N(1a), are planar with no atom deviating by more than 0.02 Å from the mean plane. All these collectively conform to the diimine formulation of the bqdi ligand.

The short Ru–N bond lengths in the above two structures indicate considerable $Ru(t_{2g})$–$L(\pi^*)$ interaction. The average of Ru–N lengths (*ca.* 1.97 Å) in the present compound compare well with Ru–N (azo) lengths (*ca.* 1.98 Å) in $[RuCl_2(pap)_2]$ [pap = 2-(phenylazo)pyridine] where very strong $\pi$ interactions have been noted.[23] On the other hand, the average Ru–$NH_3$ bond length[24] (*ca.* 2.16 Å) in $[Ru(NH_3)_5(pz)]^{2+}$ (pz = pyrazine), where there is no $\pi$ interaction, is much longer than those in **1a** and **2**. These $\pi$ interactions are also reflected in the long C–N (imine) lengths. The bond lengths in **1a** compare well with those in **2**. Notably, the average Ru–N and C–N (imine) distances in [Ru(acac)₂(diimine)] compounds are different[9] from those in $[Ru(bpy)_2(bqdi)]^{2+}$, which can be attributed to the superior $\pi$ interactions in the Ru-acac complexes. The Ru–O lengths in **1a** and **2** compare well[25,26] with those in $[Ru(acac)_2Cl_2]^-$ and $[Ru(acac)_3]$. In the present context it may be noted that examples of structurally characterized ruthenium–diimine complexes are scarce[21,27] and no compound of an unsymmetrical N-substituted diimine is known.

**Redox properties**

The redox behaviour of the diimine complexes was studied using cyclic voltammetry in acetonitrile (0.1 M $NEt_4ClO_4$). The potential range 2.0 to −1.2 V was scanned by using a platinum working electrode. For the more negative region a glassy carbon electrode was employed. All the potentials (Table 4) are referenced to a saturated calomel electrode (SCE).

The cyclic voltammogram of a typical [Ru(acac)₂L] complex displayed in Fig. 5 shows four one-electron redox processes in the potential range 2.0 to −2.5 V. Two, which are oxidative in nature, occur at positive potentials. The other two are reductive responses and appear at negative potential. Of the two redox

$$[Ru^{IV}(acac)_2L]^{2+} \xleftarrow{\quad}_{I} [Ru^{III}(acac)_2L]^+ \xleftarrow{\quad}_{II} [Ru^{II}(acac)_2L] \xleftarrow{\quad}_{III}$$

$$[Ru^{II}(acac)_2L]^- \xrightarrow{\quad}_{IV} [Ru^{II}(acac)_2L]^{2-}$$

responses *viz.* I and II, the latter is electrochemically reversible ($\Delta E_p = 100$ mV, $i_{pa} \propto v^{\frac{1}{2}}$), which has been assigned to a $Ru^{III}$–$Ru^{II}$ process. The couple I, on the other hand, is irreversible and does not show a cathodic counterpart. Since the ligand in **1** is in the oxidized diimine state it is reasonable that the anodic wave I corresponds to an irreversible oxidation, $Ru^{III} \longrightarrow Ru^{IV}$. The process at negative potentials III and IV, formally correspond to ligand reductions. The diimine ligand, L, in principle, can undergo two-step reductions. The couple III is reversible ($\Delta E_p = 100$ mV, $i_{pa} \propto v^{\frac{1}{2}}$), at least on the CV timescale, which may be attributed to the reduction diimine $\longrightarrow$ semiquinone diimine, whereas the irreversible reduction at least potential, IV, is due to further reduction of the semiquinone imine to diamine.

Interestingly, the potentials of all the redox couples (I–IV) depend linearly on the Hammett parameter,[28] $\Sigma\sigma_p$, of the substituent on L. Indeed there is quite a large change in the donor character of the ligand L in the series of **1a–1d** and an anodic shift as the electron withdrawing ability of the substituent increases (Table 4). The values of the slopes of the linear plots of $E^\circ_{298}$ *vs.* $\Sigma\sigma_p$ for the above four redox processes are: I, 0.178; II, 0.242; III, 0.302 and IV, 0.202 V. The Hammett correlation diagram for **1** has been deposited (SUP 57411). The most sig-

**Table 4** Electrochemical data[a]

|  | $E_{\frac{1}{2}}$/V $(\Delta E_p$/mV)[b] | | | |
|---|---|---|---|---|
| Compound | I | II | III | IV |
| **1a** | 1.60[c] | 0.41(90) | −1.05(90) | −2.04[d] |
| **1b** | 1.53[c] | 0.33(100) | −1.14(100) | −2.09[d] |
| **1c** | 1.48[c] | 0.27(100) | −1.17(100) | −2.15[d] |
| **1d** | 1.66[c] | 0.52(100) | −0.87(100) | −1.94[d] |
| **2** | 1.56[c] | 0.38(85) | −1.13(80) | −2.10[d] |

[a] Conditions: solvent, acetonitrile; supporting electrolyte, $NEt_4ClO_4$ (0.1 M); working electrode, platinum for processes I, II and III and glassy carbon for IV; reference electrode, SCE; solute concentration, $10^{-3}$ M. [b] $E_{\frac{1}{2}}$ is calculated as the average of anodic ($E_{pa}$) and cathodic ($E_{pc}$) peak potentials; $\Delta E_p = E_{pa} - E_{pc}$. [c] Irreversible, $E_{pa}$. [d] Irreversible, $E_{pc}$.

**Table 5** Crystallographic data for complexes **1a** and **2**

|  | **1a**·0.25H₂O | **2** |
|---|---|---|
| Empirical formula | $C_{22}H_{24.5}N_2O_{4.25}Ru$ | $C_{16}H_{20}N_2O_4Ru$ |
| $M$ | 486.01 | 405.41 |
| $a$/Å | 33.578(9) | 16.0057(17) |
| $b$/Å | 9.922(2) | 10.6005(12) |
| $c$/Å | 26.354(5) | 10.3858(12) |
| $\beta$/° | 93.11(1) | 111.069(4) |
| $U$/Å³ | 8768(3) | 1644.3(3) |
| $Z$ | 16 | 4 |
| $D_c$/mg m⁻³ | 1.473 | 1.638 |
| $R1$ [$I > 2\sigma(I)$] | 0.0799 | 0.0227 |
| $wR2$ [$I > 2\sigma(I)$] | 0.1122 | 0.0574 |
| Goodness of fit | 1.009 | 1.091 |

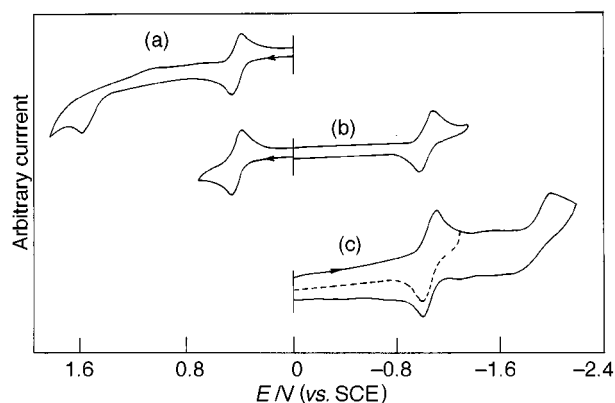Details in common: monoclinic, space group $C2/c$



**Fig. 5** Cyclic voltammogram ($v = 50$ mV s⁻¹) of complex **1a** in MeCN containing 0.1 M $NEt_4ClO_4$. Potentials are referenced to SCE: (a) at a platinum electrode, potential range 0 to +2 V; (b) at a platinum electrode, +0.8 to −1.4 V; and (c) at a glassy carbon electrode, 0 to −2.4 V; (−−−−) indicates that the scan was reversed after the first reduction wave

nificant observation from this diagram is that the dependence of the first oxidation, II, on R essentially parallels that of the first reduction potential, III. This indeed suggests considerable mixing[3,21] between metal and ligand orbitals.

The nature of the voltammogram of [Ru(acac)₂(bqdi)] **2** is very similar to that of **1** and the potentials of its couples are slightly cathodic of those for **1a**.

## Conclusion

The first isolation of a series of ruthenium complexes involving N-substituted 1,2-benzoquinone diimines has been achieved. The syntheses involve an unusual oxidative *ortho* dimerization of an aminoarene with the formation of a C–N bond. This organic transformation is promoted by ruthenium and is not

otherwise achievable. Co-ordination of two amine residues at *cis* cites is presumably the key step for the dimerization process.

The localized double bond character of the C–N (imine) and C–C bonds of the quinonoid ring reflects the diimine oxidation state of the ligand with very little ambiguity about the oxidation states of the metal ion as well as the ligands in the above complexes.

Ongoing work concerns the synthesis and characterization of diimine chelates of other transition elements.

## Experimental

### Materials

Tris(acetylacetonato) ruthenium(III) was prepared by the reported method.[29] Solvents and chemicals used for syntheses were of analytical grade. The supporting electrolyte (tetraethylammonium perchlorate) and solvents for electrochemical work were obtained as before.[30]

### Physical measurements

A Hitachi 330 spectrophotometer was used to record UV/VIS/NIR spectra in solutions. Infrared spectra were recorded with a Perkin-Elmer 783 spectrophotometer, $^1$H NMR spectra in CDCl$_3$ with a Varian VIR 300S spectrometer and SiMe$_4$ as the internal standard. A Perkin-Elmer 240C elemental analyzer was used to collect microanalytical data (C, H, N). Electrochemical measurements were done under a nitrogen atmosphere on a PAR model 370-4 electrochemistry system as reported earlier.[30] All potentials in this work are referenced to the saturated calomel electrode (SCE) and are uncorrected for junction contribution. The value for the ferrocenium–ferrocene couple under our experimental conditions is 0.42 V.

### Syntheses of complexes

The complexes were synthesized by using a general method. Details are given for a representative compound.

**Bis(acetylacetonato)(*N*-phenyl-1,2-benzoquinone diimine)ruthenium(II) [Ru(acac)$_2$L$^1$] 1a.** A sample of [Ru(acac)$_3$] (0.2 g, 0.50 mmol) was added to aniline (0.5 cm$^3$) and the mixture heated on an oil-bath at 130 °C for 90 min. The initial red colour gradually changed to intense pink. The crude product thus obtained was purified on a silica gel column (diameter, 1 cm; height, 50 cm). An intense pink band was eluted with chloroform–acetonitrile (9:1). On evaporation of the solvent and subsequent crystallization from an aqueous acetonitrile solution brown crystals were obtained. Yield, 30% (Found: C, 54.5; H, 5.1; N, 5.8. Calc. for C$_{22}$H$_{24}$N$_2$O$_4$Ru: C, 54.9; H, 5.0; N, 5.8%).

Addition of a few drops of NEt$_3$ at the beginning of the reaction facilitated it. In this case the reaction was over in about 30 min and the yield of the product also increased to 70%.

The above reaction occurs only neat. In high boiling solvents, *viz.* 2-methoxyethanol, ethylene glycol, *etc.* [Ru(acac)$_3$] failed to react with aniline. Other substituted compounds were synthesized similarly. The yields and the analytical data of the respective compounds are as follows: **1b**, 35 and 72% (NEt$_3$) (Found: C, 56.4; H, 5.6; N, 5.5. Calc. for C$_{24}$H$_{28}$N$_2$O$_4$Ru: C, 56.5; H, 5.5; N, 5.5%); **1c**, 32 and 75% (NEt$_3$) (Found: C, 53.3; H, 5.2; N, 5.1. Calc. for C$_{24}$H$_{28}$N$_2$O$_6$Ru: C, 53.2; H, 5.2; N, 5.2%); **1d**, 30 and 68% (NEt$_3$) (Found: C, 47.6; H, 4.2; N, 5.0. Calc. for C$_{22}$H$_{22}$Cl$_2$N$_2$O$_4$Ru: C, 48.0; H, 4.0; N, 5.1%).

**Bis(acetylacetonato)(*o*-benzoquinonediimine)ruthenium(II) [Ru(acac)$_2$(bqdi)] 2.** A mixture of [Ru(acac)$_3$] (0.2 g, 0.50 mmol) and 1,2-phenylenediamine (0.065 g, 0.60 mmol) in 2-methoxyethanol was heated at reflux for 6 h. The colour changed from red to pink. The solvent was evaporated on a water-bath and the solid mass purified on a silica gel column. A pink band

was eluted with chloroform–acetonitrile (20:1). On evaporation of the solvent and subsequent crystallization from dichloromethane–hexane (1:5) solution shiny red crystals were obtained. Yield 45% (Found: C, 47.6; H, 4.4; N, 7.0. Calc. for C$_{16}$H$_{20}$N$_2$O$_4$Ru: C, 47.4; H, 4.9; N, 6.9%).

### X-Ray crystallography

**(a) [Ru(acac)$_2$L$^1$]·0.25H$_2$O 1a·0.25H$_2$O.** Suitable crystals of complex **1a** for X-ray diffraction studies were obtained by slow evaporation of a saturated solution of the compound in hexane. The crystal data are given in Table 5.

Intensity data for a brown irregular crystal with dimensions 0.20 × 0.25 × 0.30 mm were measured at room temperature, 293(2) K, on an Enraf-Nonius CAD4 diffractometer equipped with graphite-monochromatized Mo-K$\alpha$ radiation, $\lambda$ = 0.710 73 Å. Cell parameters were refined[31] by a least-squares procedure on the setting angles of 25 reflections (4.5 ⩽ θ ⩽ 11.2°). The ω–2θ scan technique was employed to measure the intensities up to a maximum Bragg angle (θ) of 32.4°. No decomposition of the crystal occurred during the data collection. Corrections were applied for Lorenz-polarization effects and for absorption (μ = 0.73 mm$^{-1}$). A total of 13 038 reflections were collected, of which 12 707 were unique ($R_{int}$ = 0.1951), and of these 12 705 satisfied the $I \geqslant 2.0\sigma(I)$ criterion and were used in the subsequent analysis.

The structure was solved by direct methods[32] and refined by full-matrix least squares based on[33] $F^2$. Non-hydrogen atoms were refined with anisotropic displacement parameters. The H atoms of the ligands were located in calculated positions (C–H 0.93 and 0.96, N–H 0.86 Å) and not refined. Those of the water molecule were not located. A weighting scheme of the form $w = 1/[\sigma^2(F_o^2) + (0.0362P)^2 + 0.0000P]$ where $P = (F_o^2 + 2F_c^2)/3$ was introduced and the refinement proceeded smoothly to convergence with a maximum Δ/σ of 0.001 for 529 variables. The analysis of variance showed no special features and the maximum and minimum residual electron density peaks in the final difference map were +0.623 and −0.824 e Å$^{-3}$ respectively.

**(b) [Ru(acac)$_2$(bqdi)] 2.** An X-ray quality crystal of complex **2** was obtained by slow diffusion of a dichloromethane solution of the compound into hexane. The crystal data are collected in Table 5.

A caramel prismatic crystal with dimensions 0.30 × 0.30 × 0.25 mm was mounted on a glass fiber and used for data collection. Cell constants and an orientation matrix for data collection were obtained by least-squares refinement of the diffraction data from 25 reflections in the range 9.17 ⩽ θ ⩽ 18.34° on an Enraf-Nonius MACH3 automatic diffractometer.[34] Data were collected at 293(2) K using Mo-K$\alpha$ radiation ($\lambda$ = 0.710 73 Å) and the ω-scan technique and corrected for Lorenz-polarization effects. An empirical absorption correction was made. A total of 1762 reflections were collected, of which 1663 were unique ($R_{int}$ = 0.0111).

The structure was solved by Patterson and Fourier methods[35] which revealed the positions of all non-hydrogen atoms, and refined on $F^2$ by full-matrix least squares using anisotropic displacement parameters.[36] The asymmetric unit consists of half of the molecule which generates the other half through a crystallographic twofold axis passing through Ru(1) and bisecting bonds C(11)–C(11a) and C(13)–C(13a). All hydrogen atoms were located from Fourier-difference maps and refined isotropically. Atomic scattering factors were obtained from ref. 37. Molecular graphics from PLATON 97.[38]

CCDC reference number 186/1067.

See http://www.rsc.org/suppdata/dt/1998/2901/ for crystallographic files in .cif format.

# References

1 H. Masui, A. B. P. Lever and P. R. Auburn, *Inorg. Chem.*, 1991, **30**, 2402.
2 H. Masui, A. B. P. Lever and E. S. Dodsworth, *Inorg. Chem.*, 1993, **32**, 258 and refs. therein.
3 A. B. P. Lever, H. Masui, R. A. Metcalfe, D. J. Stufkens, E. S. Dodsworth and P. R. Auburn, *Coord. Chem. Rev.*, 1993, **125**, 317.
4 R. A. Metcalfe, E. S. Dodsworth, S. S. Fielder, D. J. Stufkens, A. B. P. Lever and W. J. Pietro, *Inorg. Chem.*, 1996, **35**, 7741.
5 F. Hartl, T. L. Snoeck, D.J. Stufkens and A. B. P. Lever, *Inorg. Chem.*, 1995, **34**, 3887.
6 L. F. Warren, *Inorg. Chem.*, 1977, **16**, 2814.
7 A. Anillo, C. Bario, S. G.-Granda and R. O.-Rosete, *J. Chem. Soc., Dalton Trans.*, 1993, 1125 and refs. therein.
8 A. M. Pyle and J. K. Barton, *Inorg. Chem.*, 1987, **26**, 3820; A. M. Pyle, Y.-M. Chiang and J. K. Barton, *Inorg. Chem.*, 1990, **29**, 4487.
9 P. Belser, A. von. Zelewsky and M. Zehnder, *Inorg. Chem.*, 1981, **20**, 3098.
10 S. Joss, K. M. Hasselbach, H. B. Buergi, R. Wordel, F. E. Wagner and A. Ludi, *Inorg. Chem.*, 1989, **28**, 1815.
11 G. M. Brown, T. R. Weaver, F. R. Keene and T. J. Meyer, *Inorg. Chem.*, 1976, **15**, 190; F. R. Keene, D. J. Salmon and T. J. Meyer, *J. Am. Chem. Soc.*, 1976, **98**, 1884.
12 K. N. Mitra, P. Majumdar, S.-M. Peng, A. Castiñeiras and S. Goswami, *Chem. Commun.*, 1997, 1267.
13 J. March, *Advanced Organic Chemistry*, 3rd edn., Wiley Interscience, New York, 1985, p. 1034; R. L. Hand and R. F. Nelson, *J. Am. Chem. Soc.*, 1974, **96**, 850; W. S. Trahanovsky, *Oxidations in Organic Chemistry*, Academic Press, New York and London, 1973, vol. 5, Part B, p. 73; D. V. Banthorpe, E. D. Hughes and C. Ingold, *J. Chem. Soc.*, 1964, 2864.
14 R. Tang, S. E. Diamond, N. Neary and F. Mares, *J. Chem. Soc., Chem. Commun.*, 1978, 562; S. E. Diamond, G. M. Tom and H. Taube, *J. Am. Chem. Soc.*, 1975, **97**, 2661; P. A. Lay, A. M. Sargeson, B. W. Skelton and A. H. White, *J. Am. Chem. Soc.*, 1982, **104**, 6161.
15 K. N. Mitra and S. Goswami, *Chem. Commun.*, 1997, 49; *Inorg. Chem.*, 1997, **36**, 1322.
16 A. A. Danopoulos, A. C. C. Wong, G. Wilkinson, M. Hursthouse and B. Hussain, *J. Chem. Soc., Dalton Trans.*, 1990, 315.
17 S. Nemeth, L. I. Simandi, G. Argay and A. Kalman, *Inorg. Chim. Acta*, 1989, **166**, 31.
18 C. Mealli and D. M. Proserpio, (*a*) CACAO, Version 4.0, July 1994; (*b*) *J. Chem. Educ.*, 1990, **67**, 399.
19 R. H. Magnuson and H. Taube, *J. Am. Chem. Soc.*, 1975, **97**, 5129.
20 G. A. Mines, J. A. Roberts and J. T. Hupp, *Inorg. Chem.*, 1992, **31**, 125.
21 C. J. da. Cunha, S. S. Fielder, D. V. Stynes, H. Masui, P. R. Auburn and A. B. P. Lever, *Inorg. Chim. Acta*, 1996, **242**, 293.
22 H. Y. Cheng and S.-M. Peng, *Inorg. Chim. Acta*, 1990, **169**, 23.
23 A. Seal and S. Ray, *Acta Crystallogr. Sect. C*, 1984, **40**, 929.
24 M. E. Gress, C. Creutz and C. O. Quicksall, *Inorg. Chem.*, 1981, **20**, 1522.
25 T. Hasegawa, T. C. Lau, H. Taube and W. P. Schaefer, *Inorg. Chem.*, 1991, **30**, 2921.
26 G. K.-J. Chao, R. L. Sime and R. J. Sime, *Acta Crystallogr., Sect. B*, 1973, **29**, 2845.
27 T. Jüstel, J. Bendix, N. M. Nolte, T. Weyhermüller, B. Nuber and K. Wieghardt, *Inorg. Chem.*, 1998, **37**, 35.
28 L. P. Hammett, *Physical Organic Chemistry*, 2nd edn., McGraw-Hill, New York, 1970; R. N. Mukherjee, O. A. Rajan and A. Chakravorty, *Inorg. Chem.*, 1982, **21**, 785.
29 A. Endo, M. Watanbe, S. Hayashi, K. Shimizu and G. P. Sato, *Bull. Chem. Soc. Jpn.*, 1978, **51**, 800.
30 S. Choudhury, A. K. Deb and S. Goswami, *J. Chem. Soc., Dalton Trans.*, 1994, 1305.
31 B. A. Frenz, CAD4 SDP, in *Computing in Crystallography*, eds. H. Schenk, R. Olthof-Hazekamp, H. Van Koningsveld and G. C. Bassi, Delft University Press, 1985, pp. 64–71.
32 G. M. Sheldrick, SHELXS 86, Program for the solution of crystal structures, University of Göttingen, 1986.
33 G. M. Sheldrick, SHELXL 93, Program for the refinement of X-ray structures, University of Göttingen, 1993.
34 B. V. Nonius, CAD4-Express Software, Version 5.1/1.2, Enraf-Nonius, Delft, 1994.
35 G. M. Sheldrick, *Acta. Crystallogr., Sect. A*, 1990, **46**, 467.
36 G. M. Sheldrick, SHELXL 97, Program for the Refinement of Crystal Structures, University of Göttingen, 1997.
37 *International Tables for X-Ray Crystallography*, Kluwer, Dordrecht, 1995, vol. C.
38 A. L. Spek, *Acta Crystallogr., Sect. A*, 1990, **46**, C-34.